OPEN ACCESS
Jurnal Ilmiah Ilmu Terapan Universitas Jambi
Vol. 10 No. 1. Ferbruary 2026, pp. 471-483 DOI. 10.22437/jiituj.v10i1.53386
Research Article

APPLYING ELECTRICAL RESISTIVITY TOMOGRAPHY FOR AGRICULTURAL LAND ASSESSMENT TO SUPPORT CROP SELECTION: A CASE STUDY IN RUMAH TIGA VILLAGE, MALUKU

Wahyudi Widyatmoko Parnadi[1,*], Grace Tuhumury[2], Samsul Bahri[2]

[1] Department of Geophysical Engineering, Bandung Institute of Technology, Jawa Barat, Indonesia
[2] Department of Geophysical Engineering, Pattimura University, Maluku, Indonesia
Corresponding author email: wahyudi.parnadi@itb.ac.id

Article Info
Received: Dec 19, 2025
Revised: Jan 14, 2026
Accepted: Feb 22, 2026
OnlineVersion: Feb 24, 2026

Abstract
The declining productivity of the agricultural sector in Maluku Province poses a serious challenge, partly due to the limited availability of scientific data on agricultural land characteristics to support precision agriculture. This study aimed to develop a subsurface resistivity model and evaluate farmland suitability in Rumah Tiga Village, Ambon Island, Maluku. Electrical Resistivity Tomography (ERT) with the Wenner configuration was applied along eight survey lines, supported by laboratory analyses of porosity, water content, specific gravity, soil texture, and pH. The modelling results revealed three major resistivity zones: water-saturated clay (<20 Ωm), sandy gravel (20–33.8 Ωm), and boulders (>70 Ωm). The distribution map of soil parameters showed significant spatial variability, and further analysis demonstrated clear relationships between resistivity data and soil physical properties. Land suitability evaluation identified three classifications based on crop water requirements, covering a total area of 6,684 m²: Area I (46.72%, 3,123 m²), suitable for crops with high water demand such as rice and leafy vegetables; Area II (23.78%, 1,971 m²), suitable for crops with medium water demand such as tomatoes, chillies, and corn; and Area III (29.50%, 1,590 m²), suitable for crops with low water demand such as tubers and legumes. This research provides a scientific basis for sustainable agricultural planning and the implementation of precision agriculture in Ambon and its surrounding areas.

Keywords: Electrical Resistivity Tomography, ERT, Precision Agriculture, Soil Characterization, Wenner Configuration.

© 2026 by the author(s)
This article is an open access article distributed under the terms and conditions of the Creative Commons Attribution (CC BY) license (https://creativecommons.org/licenses/by/4.0/).

INTRODUCTION

Agriculture is a strategic sector that plays a pivotal role in ensuring food security and driving economic growth, particularly in resource-rich regions such as Indonesia. In Maluku Province, however, agricultural productivity has been declining (BPS, 2024). This decline is attributed to climate change, land degradation, and the limited application of modern agricultural technologies (Syabawaihi et al., 2025). Moreover, a lack of understanding of soil characteristics further contributes to the problem,

although soil is the primary medium for plant growth, enabling nutrient and air absorption as well as providing space for root development (Hillel, 1982). Therefore, the adoption of precision agriculture based on soil data represents a promising approach for achieving sustainable optimization of production.

Precision agriculture is defined as an agricultural approach that employs information and technology to optimize production (Zhang & Wang, 2020). Its primary objective is to improve the efficiency of agricultural inputs, such as water and fertilizers, while maximizing crop yields and minimizing environmental impacts (Widodo, 2023). The use of data-driven technologies, including the characterization of soil physical properties, is essential for advancing precision agriculture, particularly in developing management strategies tailored to local conditions.

The physical characteristics of soil, including porosity, water content, bulk density, texture, and pH, significantly influence land productivity. Porosity reflects the soil's capacity to retain water and accommodate air, whereas bulk density indicates soil compaction, which affects root development and water movement (Klute, 1986). Soil texture, defined by the proportions of sand, silt, and clay, plays a critical role in water and nutrient retention (Alghamdi et al., 2023; Hillel, 1982). Likewise, soil pH determines nutrient bioavailability for plants and regulates microbial activity within the soil matrix. Conventional methods for assessing soil characteristics, however, demand considerable time, financial resources, and labor. As a result, geophysical techniques have attracted increasing attention. Electrical resistivity methods have been widely employed due to their cost-effectiveness, scalability, and suitability for two-dimensional dynamic monitoring (Zhao et al., 2020; Bahri et al., 2023). Their effectiveness relies on the principle of resistivity, which enables the lateral and vertical characterization of subsurface lithology (Reynolds, 1997). Moreover, they provide a reliable, non-invasive alternative for determining soil physical properties. Previous studies, such as Widodo et al. (2023) in Cidadap, West Java, demonstrated the effectiveness of integrating ERT and electromagnetic methods in delineating soil structure without disturbing the terrain. Similarly, Hovhannissian et al. (2019) in South Africa reported a strong correlation between soil resistivity and soil fertility parameters. These findings highlight the potential of geophysical methods to support sustainable agriculture.

This study was conducted in Rumah Tiga Village, Ambon City, Maluku. The location was selected due to the urgent need to enhance agricultural production in the region, compounded by the limited availability of soil characteristic data that could serve as a reference for land-use planning. This study aims to determine the soil characteristics of agricultural land by applying the Wenner configuration of electrical resistivity tomography (ERT) and integrating it with soil physical parameters such as porosity, water content, bulk density, texture, and pH. The integration between ERT and the measurement of soil physical parameters is the strength and novelty of this research. Previously, the mapping of land characteristics was only based on the measurement of soil samples carried out in the laboratory. The use of the ERT method has the advantage that the observed area is wider, faster, and the cost is more affordable. This approach enables the evaluation of land suitability, thereby supporting the selection of appropriate crops and more efficient land management. The results are expected to provide a scientific reference for farmers, government agencies, and researchers in decision-making related to land management and data-driven agricultural development. Furthermore, the study highlights the potential of geophysical technology in agriculture, particularly in regions that remain underexplored.

RESEARCH METHOD

The study was conducted from August 2024 to February 2025. Geoelectric measurements were carried out using the Electrical Resistivity Tomography (ERT) method with a Wenner configuration. The selection of this configuration over others is due to its high signal strength, which results in more accurate data. Additionally, in 2D surveys, the Wenner array produces stable and smooth inversion models, especially for simple geological structures that are not highly complex laterally (Niaz et al., 2021). The inversion process with RES2DINV tends to converge quickly because the data has good consistency. Eight measurement lines were established, with lengths of 42 m for lines 1–7 and 30 m for line 8, and an electrode spacing of 1 m (see Figure 1). Measurements were obtained using a Naniura FRD 300 Plus geoelectric instrument with current and potential electrodes connected. The main principle of this method is to inject high-voltage direct current into the ground through two current electrodes, and then measure the voltage response using two potential electrodes (Bahri et al., 2025). The apparent resistivity value is obtained from the geometric constant, current, and measured potential difference for each datum. Data processing was performed using RES2DINV software to generate two-dimensional subsurface cross-sections, which were subsequently integrated into SketchUp software to construct a quasi-three-

dimensional model. A full three-dimensional cross-section was then developed using Rockworks20 software.

Mathematically, the inversion process is fundamentally an optimization problem aimed at finding a subsurface resistivity distribution model that can generate calculated data which closely matches the field observation data. This process begins with the creation of a simple initial model that has a uniform resistivity value, usually the logarithmic mean of all field data. This model then undergoes a series of iterations aimed at minimizing a complex objective function. To update the model at each iteration, this inversion uses a least-squares approach by utilizing the Jacobian matrix or sensitivity matrix, which can be accurately calculated using the Gauss-Newton method or estimated using the faster Quasi-Newton method. This iterative process will continue and stop when the convergence criteria are met, indicated by the Root-Mean-Squared (RMS) error value no longer showing a significant decrease between iterations, suggesting that the model has reached its most optimum condition and is ready for geological interpretation (Loke & Dahlin., 2002).

To obtain representative soil samples, 20 points were selected along the geoelectric measurement lines (Figure 1). Sampling was conducted using a ring soil sampler, with samples collected from a depth of 10–30 cm. The soil was placed in clean plastic bags and transported to the laboratory for analysis. The physical parameters tested included porosity, water content, bulk density, soil texture, and pH. For porosity and water content analysis, samples were weighed to determine wet weight, then oven-dried at 105°C for 24 hours until a constant dry weight was achieved. Porosity and water content were calculated using dry weight and soil volume. Bulk density was determined as the ratio of dry soil weight to the ring sampler volume. For soil texture analysis, dried samples were sieved using mesh sizes 40, 60, and 200 to determine the proportions of sand, silt, and clay. Soil pH was measured by inserting a pH meter into a moist soil sample.

Based on the regional geological map in Figure 1, the research area is a combination of ancient volcanic rocks that have undergone uplift and faulting, which are then covered by carbonate units (coral), and finally by alluvial sedimentation processes along the coastline of Ambon Bay. The Ambon Volcanic Rocks (Tpav) are the oldest formation in this area (colored orange). They consist of igneous and pyroclastic rocks such as Andesite, Dacite, Breccia, and Tuff. These rocks form the mountain or hill framework in the northern, western, and southern parts of the research area. The Coral Limestone (Ql) consists of coral colonies, algae, and bryozoa. The presence of this limestone indicates that the area was once a shallow marine environment that was subsequently uplifted to the surface. The Alluvium (Qa) is the youngest deposit (colored yellow), consisting of loose materials such as pebbles, gravel, sand, silt, and clay. These deposits are concentrated in the lowlands near the coast of Ambon Bay, resulting from the erosion of upstream rocks transported by river flows (Pownall et al., 2013).

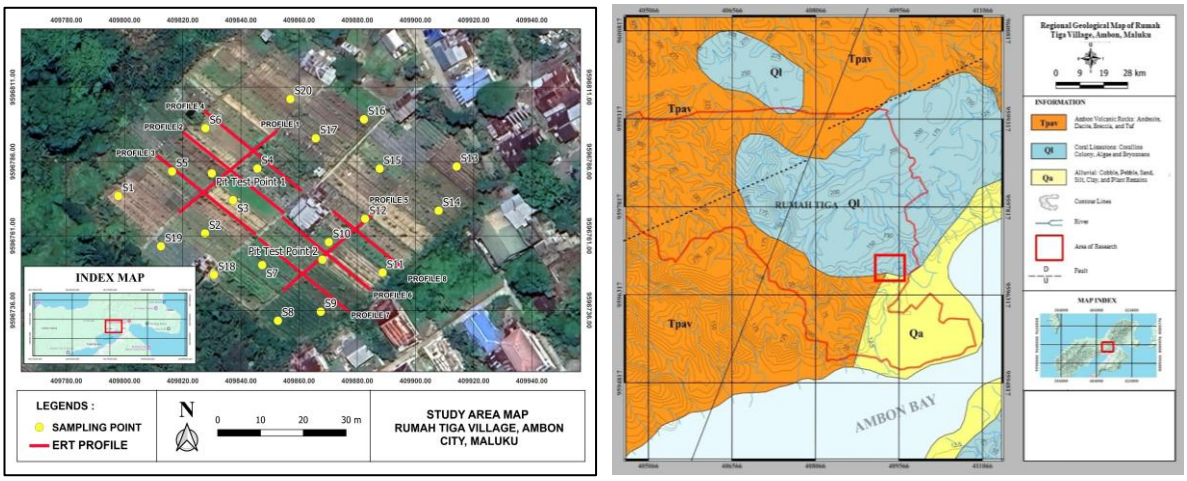

Figure 1. Research Location Area in Rumah Tiga Village, Ambon City and Regional Geological of Study Area

RESULTS AND DISCUSSION

ERT Measurement Results

Geoelectric measurements were carried out along eight lines in agricultural land at Rumah Tiga Village, Ambon City, with line lengths ranging from 30 to 42 m and an inter-electrode spacing of 1 m.

The 2D modelling results obtained using the Electrical Resistivity Tomography (ERT) method with a Wenner configuration revealed variations in subsurface resistivity values. The resistivity values ranged from 20 to 70 Ωm. Layer interpretation was performed based on the following criteria: resistivity values below 20 Ωm indicate water-saturated clay; values between 20 and 33.8 Ωm correspond to sandy gravel; and values above 70 Ωm represent boulders or hard rocks. Aquifers with resistivity values lower than 10 Ωm were also identified. The distribution of resistivity values demonstrates the heterogeneity of the soil at the study site, both vertically and laterally. Figure 2 - 9 presents the inversion results of ERT data for the eight survey lines.

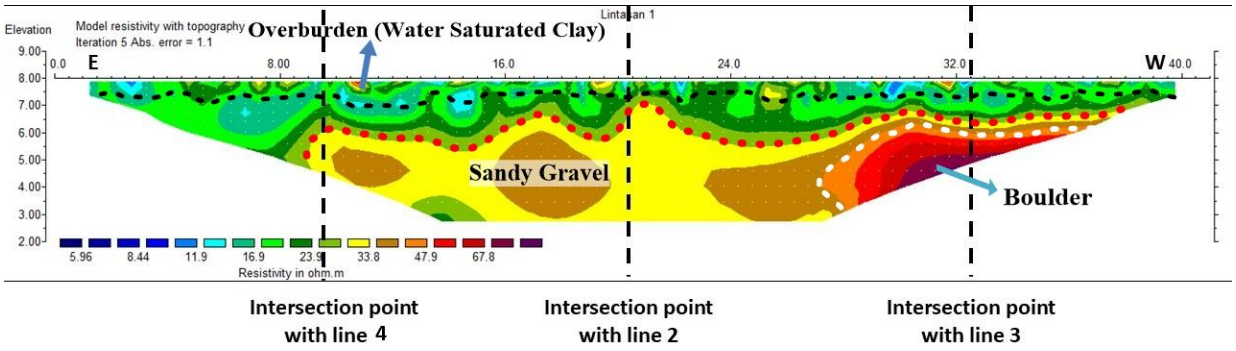

Figure 2. Cross-section Modeling of Line 1

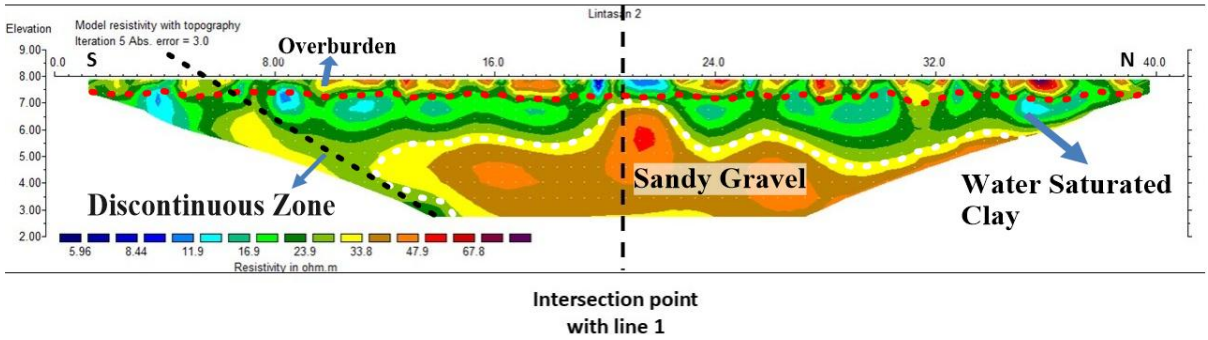

Figure 3. Cross-section Modeling of Line 2

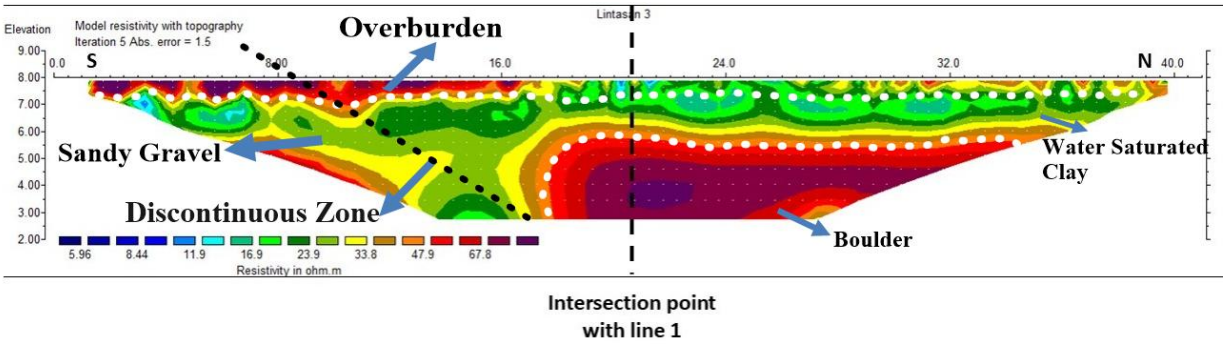

Figure 4. Cross-section Modeling of Line 3

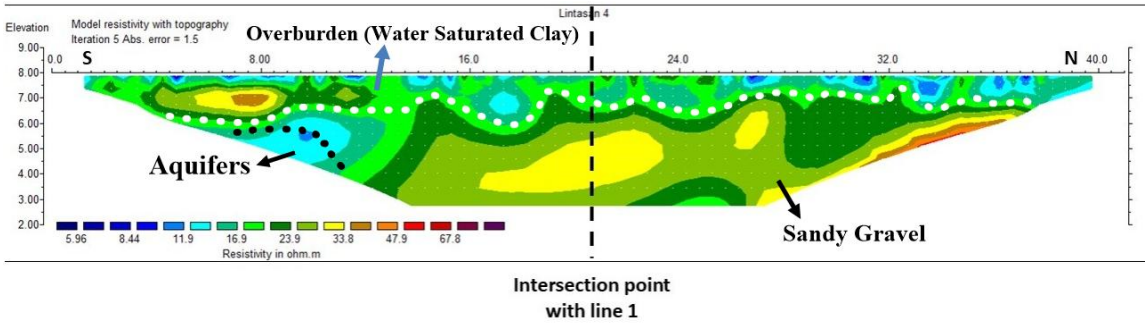

Figure 5. Cross-section Modeling of Line 4

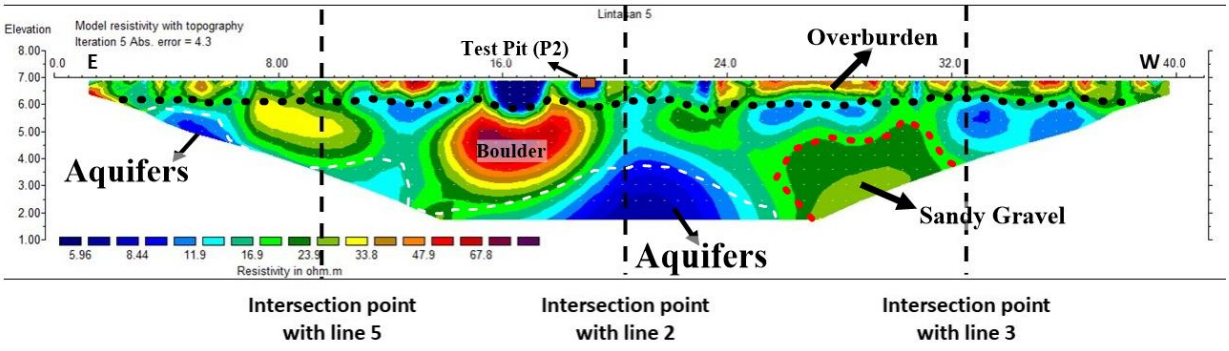

Figure 6. Cross-section Modeling of Line 5

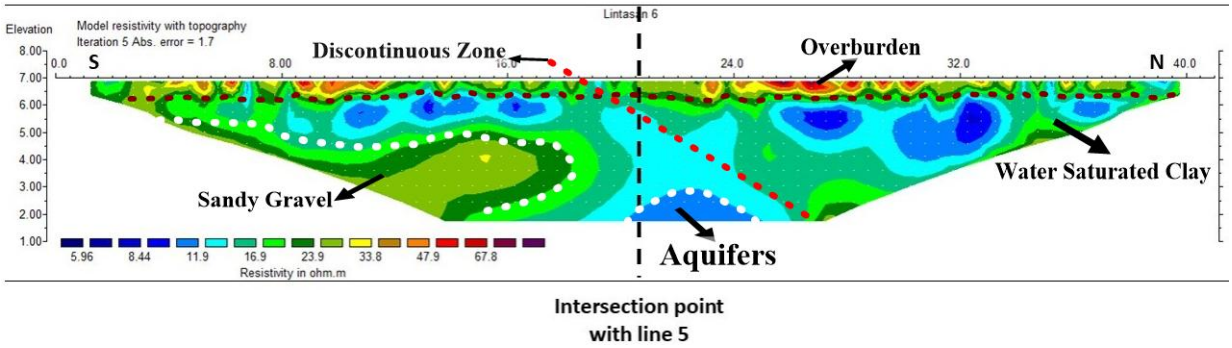

Figure 7. Cross-section Modeling of Line 6

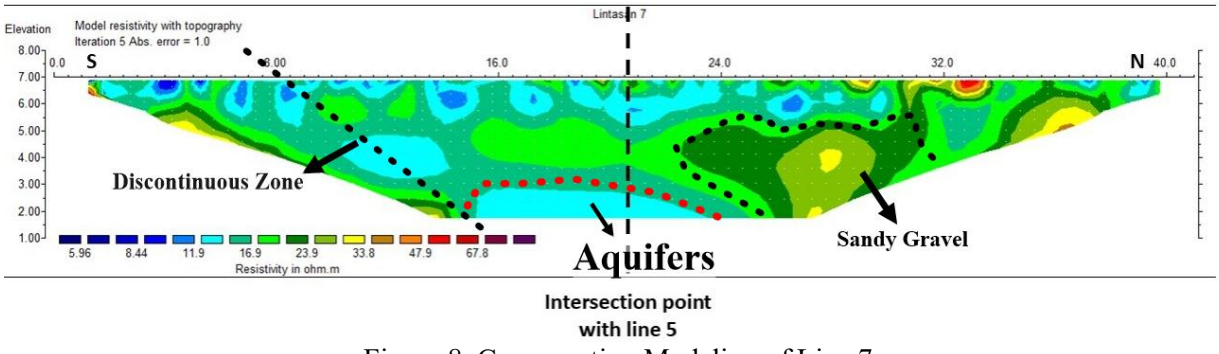

Figure 8. Cross-section Modeling of Line 7

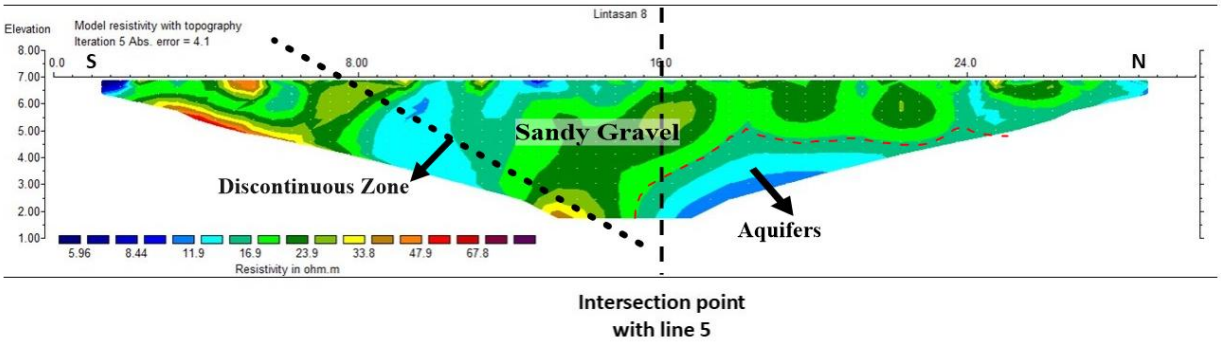

Figure 9. Cross-section Modeling of Line 8

Quasi 3D Modeling of ERT Measurement Results

The quasi-3D approach in ERT involves acquiring 2D resistivity data along multiple adjacent lines and integrating them to construct a three-dimensional subsurface model. This method provides a more comprehensive representation of lateral and vertical variations in subsurface resistivity (Cheng et al., 2019). Figure 10 presents the quasi-3D model for the study area. As shown, lines 1–4 exhibit higher resistivity values than lines 5–8, indicating lower conductivity in these zones. By applying 3D modeling

like this, we can determine the distribution of the thickness of the upper humus-rich soil layer, which is typically characterized by low resistivity values. The relatively wide spacing between lines creates limitations in interpolation, so it cannot cover the entire research area.

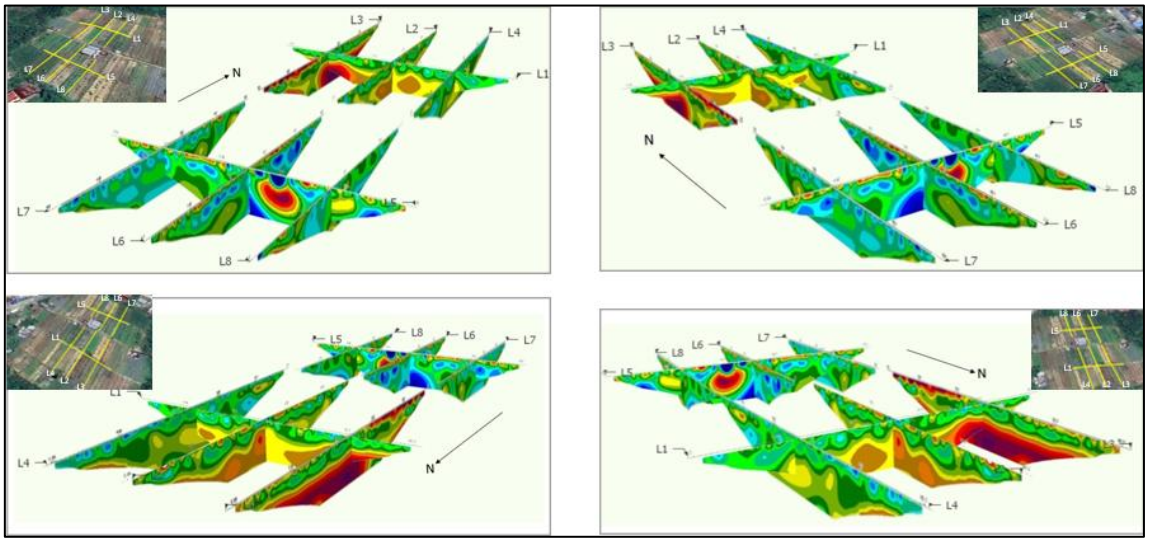

Figure 10. Quasi 3D Modeling of ERT Measurements

Results of Soil Physical Parameter Measurements

The analysis of soil physical parameters from 20 sampling points in the agricultural land of Rumah Tiga Village revealed distinct spatial variations across the study area. These were visualised through a colour-scaled distribution map (Figure 11).

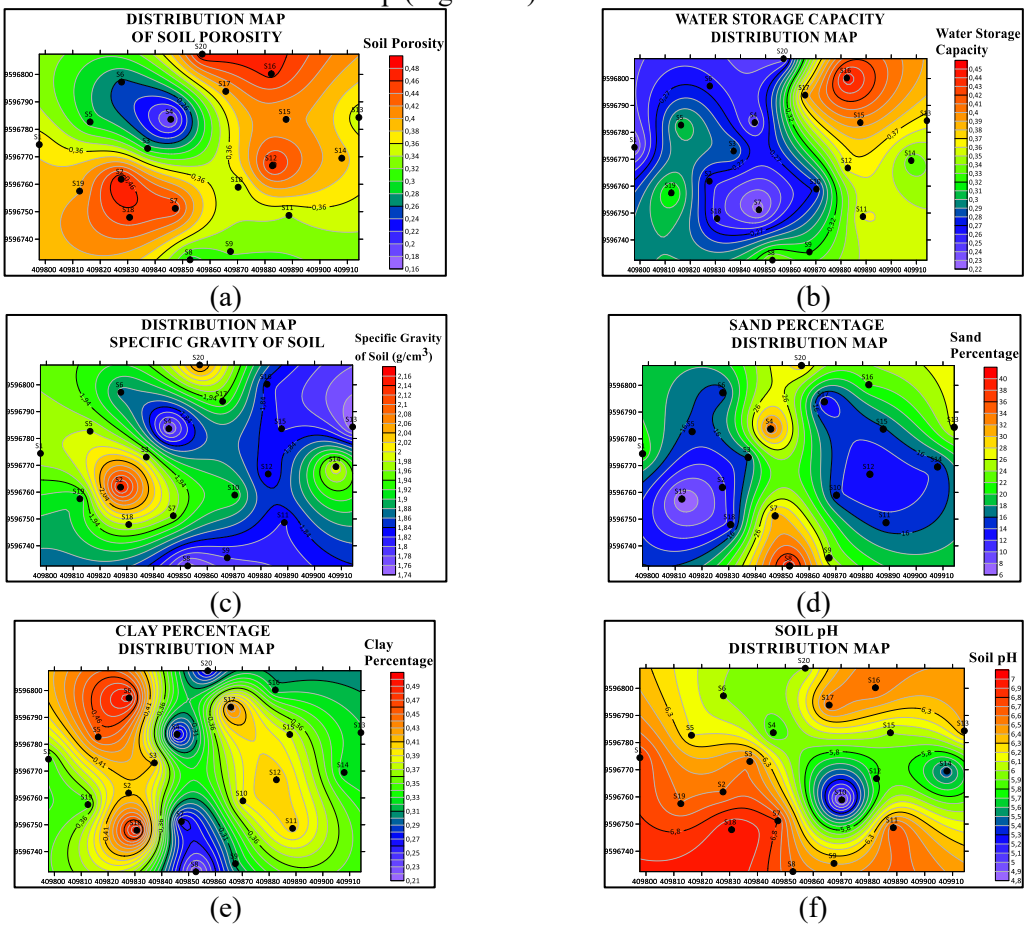

Figure 11. Results of Physical Parameter Distribution Maps (a) Soil Porosity Distribution Map, (b) Water Storage Capacity Distribution Map, (c) Soil Specific Gravity Distribution Map, (d) Sand Percentage Distribution Map, (e) Clay Percentage Distribution Map, (f) Soil pH Distribution Map.

The porosity distribution map indicates that areas with high porosity values (red and orange) possess larger pore spaces, allowing rapid water infiltration but limiting water storage capacity, which leads to faster dissipation of soil moisture despite the presence of residual oxygen. Conversely, areas with low porosity values (blue and green) have smaller pore spaces that impede infiltration yet promote greater soil moisture retention (Sonora et al., 2022; Dermawan et al., 2022). Optimal porosity for plant growth is generally considered to range between 40% and 60% of total porosity, as this provides sufficient space for both water and air storage (Cai et al., 2023). In addition, adequate macropores (>1 mm) are necessary to facilitate water flow and oxygen uptake by roots (Wang & Zhang, 2024). Excessive soil compaction, however, may restrict root development due to oxygen deficiency. As shown in Figure 11(a), sample points S4 and S6 exhibit the lowest porosity values. At S6, this condition is mainly attributable to high clay content, whereas at S4, despite a high sand fraction and overall high porosity, the pore structure is unstable, resulting in rapid infiltration. Both areas were also subjected to intensive watering during sampling, which likely filled the pores with water and reduced effective porosity (Taruna et al., 2021). The problem of low porosity can be mitigated through the incorporation of organic matter, which has been demonstrated to increase both total porosity and macroporosity. Furthermore, the use of heavy machinery should be minimised under high soil moisture conditions to prevent compaction and ensure the maintenance of optimal porosity.

The distribution map of air storage capacity (Figure 11 (b)) shows a gradation from blue (low) to red (high), with orange to red regions representing high capacity. Such areas can support soil moisture during the dry season and enhance photosynthesis, nutrient uptake, and root growth (Liu et al., 2024). By contrast, blue to green regions exhibit low air storage capacity, requiring additional soil management practices such as improved irrigation. This spatial variability is hypothesised to result from differences in lithology and topography. High-capacity areas are generally associated with clay-rich soils, which retain more air compared to sandy soils (Astriani et al., 2022), and are located at higher elevations with effective drainage that promotes rapid runoff (Amalia & Suriamihardja, 2019). Groundwater depth also plays a role; high-capacity zones are typically underlain by deeper water tables, whereas shallow water tables in low-capacity areas reduce air-filled porosity, as indicated by aquifer signatures in the 2D resistivity cross-sections (Figures 6–9). Management interventions to enhance air storage in low-capacity areas include the application of organic or plastic mulch to reduce evaporation and maintain humidity, as well as the incorporation of organic matter, which has been demonstrated to increase soil air storage capacity (Lopes et al., 2025).

The distribution map of soil specific gravity (Figure 11(c)) shows values ranging from 1.74 g/cm³ to 2.16 g/cm³, influenced by organic matter content, mineral composition, and soil moisture. Low specific gravity is generally associated with higher organic matter, which improves soil aggregation and nutrient availability (Crnobrna et al., 2022). In contrast, high specific gravity indicates denser soils that restrict air and water movement, thereby limiting root development. Sample points S2, S14, and S20 exhibit elevated specific gravity, likely due to reduced organic matter or compaction from anthropogenic activities (Iqbal et al., 2006; Saputra et al., 2018). To alleviate this condition, periodic tillage or loosening can be employed to reduce bulk density and improve soil structure. Additionally, compaction should be avoided when the soil is moist, as this state increases susceptibility to particle aggregation and pore collapse under external pressure (Orzech et al., 2021).

Figures 11(d) and 11(e) illustrate the spatial distribution of sand and clay fractions across the study area. Sand-rich regions (red to orange) are characterized by improved drainage but limited water retention (Farooq et al., 2024), whereas clay-rich regions indicate denser soils with greater capacity to retain water. The maps also reveal local anomalies in both fractions, reflecting significant textural heterogeneity in the field. These variations directly affect water retention, aeration, and other soil physical properties that influence crop suitability. While clay soils are generally more favorable for agriculture due to their moisture-holding capacity, sandy soils require more intensive water management to compensate for rapid drying.

The soil pH distribution map (Figure 11(f)) shows spatial variation ranging from acidic (blue) to alkaline (red) conditions. Optimal soil pH for most crops lies between 7.0 and 7.5 (Havlin et al., 2014), although this range varies by crop species. Localised low-pH anomalies were observed at sample points S10 and S14, likely influenced by the application of nitrogen fertilisers, which are known to acidify soils (Liu et al., 2024; Buthelezi & Buthelezi-Dube, 2023). To mitigate soil acidification, the incorporation of organic ash, lime (dolomite or calcite), and organic amendments such as compost or manure has been shown to increase pH and improve soil buffering capacity (Murni, 2009; Syahputra et al., 2024).

Conversely, overly alkaline soils may be corrected through the application of sulfur or sulfuric acid, or by irrigation with slightly acidic water, thereby restoring conditions conducive to plant growth (Liu et al., 2024).

Relationship between Resistivity Values and Soil Physical Parameters

The three-dimensional cross-section (Figure 12) was generated by interpolating eight two-dimensional profiles using the Inverse Distance Weighting (IDW) method in RockWorks20. This model provides a comprehensive visualisation of subsurface resistivity and enables interpretation of its relationship with soil physical parameters (Rupesh et al., 2024). For detailed analysis, slices were extracted at depths of 0.75 m (Figure 12(a)) and 1 m (Figure 12(b)) to examine horizontal variations in resistivity.

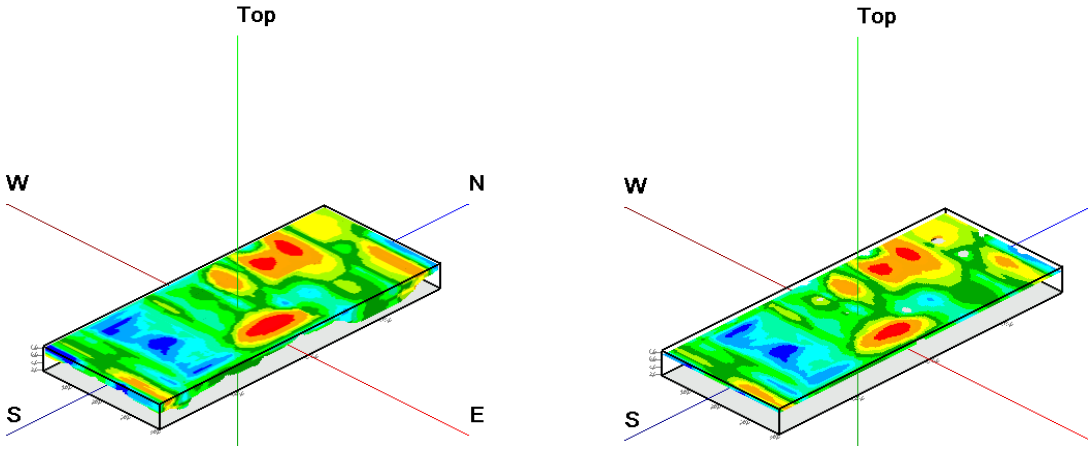

(a) (b)

Figure 12. (a) 3D Cross-Section, (b) 3D Cross-Section Slicing Depth 0.75 m

The results of the cross-sectional slicing at a depth of 0.75 m and 1 m show that the area in the north has a resistivity value that tends to be higher than the area in the south. Based on the analysis of soil physical parameters, the northern area has low to moderate porosity (Figure 11(a)), high soil specific gravity (Figure 11(c)), and low water storage capacity (Figure 11(b)). In contrast, the southern area shows a lower resistivity value, with relatively higher porosity, lower soil specific gravity, and high-water storage capacity. Based on these results, it can be concluded that the resistivity value has a unidirectional relationship (directly proportional) with soil specific gravity, but inversely proportional to porosity and water storage capacity.

The analysis indicates that soil resistivity increases with higher bulk density. This is because greater density reduces pore space between soil particles (Memon et al., 2024). Smaller pores lower the soil's capacity to retain water and air, and since water is the primary conductor in soil, reduced pore connectivity impedes current flow and raises resistivity (Salufu et al., 2022). Conversely, resistivity is inversely related to porosity and water storage capacity: a higher number of pores enhances water retention, improves conduction pathways, and thus decreases resistivity (Jusoh et al., 2022; Akintorinwa et al., 2018; Abidin et al., 2013).

Relationship between Soil Physical Parameters and Resistivity Values to Agricultural Land Suitability

Based on the results of the ERT measurements and soil physical parameters, the layer from the surface to a depth of 1 m along the research transect is identified as an overburden layer with varying resistivity values. These variations are attributed to differences in lithology, water content, and mineral composition; clay and saturated zones yield low resistivity, whereas dry and sandy formations exhibit high resistivity (Aizebeokhai, 2010). Agricultural activities such as irrigation, plowing, and the application of fertilizers and chemicals also influence resistivity values (Doni et al., 2021; Santoso et al., 2015). The upper/northern lines (1 to 4) reveal heterogeneous overburden conditions and indicate several layers, namely <20 Ωm interpreted as water-saturated clay; 20–33.8 Ωm as sandy gravel; and >70 Ωm as boulders or rock fragments. This interpretation is corroborated by a 30-cm-deep pit test, which shows a gradation of soil texture from fine material to gravelly sand.

Furthermore, the physical soil parameter map (Figure 11) corroborates the ERT results, showing that lines 1–4 exhibit high soil density (Figure 11 (c)), indicating the dominance of the sand fraction. This finding is consistent with Putra et al. (2023), who reported that coarse particles result in higher density. The sand content (Figure 11(d)) and porosity (Figure 11(a)) in this area are also classified as moderate to high, causing rapid water loss and drier soil conditions. This phenomenon is consistent with the theoretical frameworks of Brady and Weil (2002) and Hillel (1980), which suggest that sandy soils with larger particles facilitate greater water flow compared to dense clay soils. Therefore, the cultivation of drought-tolerant crops is recommended in this region, given the soil's rapid drying and efficient drainage.

In lines 5–8, located in the southern part of the research area (Figure 1), the measurements indicate more conductive conditions, with resistivity values of less than 20 Ωm starting from a depth of 50 cm. These values suggest the presence of water-saturated clay. This interpretation is corroborated by a 30-cm-deep pit test on line 5 (19 m from the zero-point electrode), which shows that with increasing soil depth, grain size decreases (Figure 6), consistent with the observed decline in resistivity. The soil physical parameter map also indicates low bulk density in this area (Figure 11 (c)), implying a higher water storage capacity (Agus and Subiksa, 2008). Furthermore, the percentage of clay is notably high (Figure 11(e)), indicating the dominance of clay fractions in the southern region. The clay layer in this area appears thicker than in the north, likely due to variations in sediment accumulation, environmental conditions, geological structures, and the downslope transport of fine materials from the higher northern areas.

Furthermore, the geoelectric cross-sections of lines 5–8 reveal the presence of shallow aquifers, delineated by light to dark blue zones with very low resistivity values. The existence of these aquifers is supported by nearby wells, which indicate groundwater levels at a depth of approximately 90 cm. This evidence corroborates the hypothesis that the southern area contains higher groundwater content than other parts of the site. The southern region is dominated by clay soil with high water storage capacity, making it well-suited for the cultivation of crops with high water requirements.

Plant Recommendations

Based on resistivity data and soil physical parameters, the research area can be divided into three zones based on groundwater storage capacity, each of which is recommended for different types of plants according to their water needs:

a) Plants with high water requirements (water > 700 mm/season, 100% requirement), such as rice, sugarcane, and green vegetables, are suitable for planting in areas with high water storage capacity because their shallow root systems require a stable water supply.
b) Plants that require moderate amounts of water (400–700 mm per season and 50–100% of their water needs), such as tomatoes, chilies, corn, and cucumbers, are suitable for areas with moderate humidity when provided with regular irrigation.
c) Plants with low water requirements (< 400 mm/season, requirement < 50%), such as cassava, sweet potatoes, and beans, are suitable for areas with low water storage capacity because they can survive in dry conditions.

Based on the data, it can be used to create a map of recommended plant types that are suitable for the area. The distribution map of recommended plants can be seen in Figure 15.

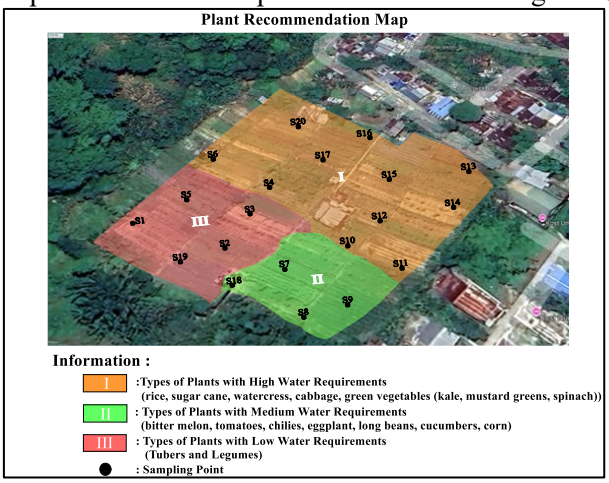

Figure 13. Recommended Plant Type Map Based on Soil Resistivity and Physical Parameter Data

Area I, covering 46.72% of the site (3,123 m²), is characterised by high conductivity, high water storage capacity, moderate porosity, and clay dominance. Area II, representing 23.78% (1,590 m²), exhibits high conductivity, moderate water storage capacity, and moderate porosity, with sand as the dominant material. Area III, covering 29.50% (1,971 m²), shows low conductivity (resistive), low water storage capacity, and low porosity.

CONCLUSION

This study characterised agricultural land in Rumah Tiga Village, Ambon City, Maluku, using the electrical resistivity tomography (ERT) method with a Wenner configuration. Eight survey lines were employed, each 42 m in length with 1 m electrode spacing. Based on the results, the following conclusions can be drawn. ERT measurements create different layers that can be understood; specifically, layers with resistivity values less than 20 Ωm are recognized as air-saturated clay, those between 20 and 33.8 Ωm are sandy gravel, layers over 70 Ωm are boulders or large rocks, and resistivity values under 10 Ωm suggest the presence of aquifers.

Based on the results of soil physical parameter measurements, which are then integrated with resistivity data, a plant recommendation map is produced with three classifications based on plant water requirements. Area I is considered suitable for cultivating plants that require a lot of water, such as rice, sugarcane, watercress, cabbage, and green vegetables such as kale, mustard greens, and spinach. This area has a soil bulk density value that is classified as low to moderate (1.75 - 1.9 g/cm³), with a percentage of medium to high soil pore space (34 - 48%), and a soil acidity level (pH) that is in the ideal range, which is between 5.8 and 6.8. Meanwhile, Area II is recommended for plants with moderate water requirements, such as bitter melon, tomatoes, chilies, eggplants, long beans, cucumbers, and corn. The soil in Area II has a specific gravity value that is also considered low to moderate (1.75–1.96 g/cm³), with soil pore space ranging from 28% to 45% and a pH level that is still ideal, between 6.6 and 7. And for Area III, it is more suitable for plants that require low amounts of water, such as tubers (cassava, sweet potatoes, and taro) and legumes (peanuts and green beans). This area is characterized by a high specific gravity value, namely between 1.98 and 2.15 g/cm³, has a percentage of moderate to high pore space (37–48%), and a pH level that remains ideal in the range of 6.6–6.8.

ACKNOWLEDGMENTS

In the implementation of this research, the task of the section is to all members of the research team. The first author (Parnadi), as the main researcher, is responsible for all stages of the research, especially in the planning process and interpretation of research results. The second author (Tuhumury) and the third author (Bahri), as members of the research team, are responsible for the acquisition of research data and also assist in the interpretation and analysis of research results.

AUTHOR CONTRIBUTIONS

Author 1 creates articles and creates instruments and is responsible for research author 2-3 analyzes research data that has been collected, author 4 assist in research data analysis, instrument validation, and input research data.

CONFLICTS OF INTEREST

The author(s) declare no conflict of interest.

USE OF ARTIFICIAL INTELLIGENCE (AI)-ASSISTED TECHNOLOGY

The authors declare that no artificial intelligence (AI) tools were used in the generation, analysis, or writing of this manuscript. All aspects of the research, including data collection, interpretation, and manuscript preparation, were carried out entirely by the authors without the assistance of AI-based technologies.

REFERENCES

Abidin, M. H. Z., Ahmad, F., Wijeyesekera, D. C., Saad, R., & Baharuddin, M. F. T. (2013). Soil resistivity measurements to predict moisture content and density in loose and dense soil. *Applied Mechanics and Materials*, 353, 911-917.

Agus, F. dan Subiksa, I. G. M. (2008). *Lahan Gambut: Potensi Untuk Pertanian Dan Aspek Lingkungan [Peatlands: Potential for Agriculture and Environmental Aspects].* Balai Penelitian Tanah.

Aizebeokhai, A. P. (2010). 2D and 3D geoelectrical resistivity imaging: Theory and field design. *Scientific Research and Essays*, 5(23), 3592-3605. https://doi.org/10.5897/SRE10.1036.

Akintorinwa, O. J., & Oluwole, S. T. (2018). Empirical relationship between electrical resistivity and geotechnical parameters: a case study of Federal University of Technology campus, Akure SW, Nigeria. *NRIAG Journal of Astronomy and Geophysics*, 7(1), 123-133.

Alghamdi, A. G., Majrashi, M. A., & Ibrahim, H. M. (2023). Improving the physical properties and water retention of sandy soils by the synergistic utilization of natural clay deposits and wheat straw. *Sustainability*, *16*(1), 46. https://doi.org/10.3390/su16010046.

Amalia, R. R., Sakka, S., & Suriamihardja, D. A. (2019). Distribusi Pengaliran Presipitasi Berdasarkan Topografi. *Jurnal Geocelebes*, *3*(2), 90-96. https://doi.org/10.20956/geocelebes.v3i2.7088.

Astriani, D. U., Muslim, D., Mulyo, A., & Pramudyo, T. (2022). Potensi tanah mengembang berdasarkan kadar lempung di Kabupaten Bekasi, Jawa Barat [Potential for soil expansion based on clay content in Bekasi Regency, West Java]. *Jurnal Goeminerba,* 7 (3): 133-141.

Bahri, S., Ramadhan, A., Zulfiah., (2023). Investigation of groundwater quality using vertical electrical sounding and dar zarrouk parameter in Leihitu, Maluku, Indonesia. *Journal of Geoscience, Engineering, Environment, and Technology*, *8*(3), 221–228. https://doi.org/10.25299/jgeet.2023.8.3.12976.

Bahri, S., Ramadhan, A., & Patty, P. J. (2025). Adaptive Flower Pollination Algorithm (FPA) for Vertical Electrical Sounding (VES) Inversion Modelling: S. Bahri et al. *Pure and Applied Geophysics*, *182*(10), 4097-4111. https://doi.org/10.1007/s00024-025-03799-8.

Brady, N. C., & Weil, R. R. (2002). The nature and properties of soils. Pearson Education

Buthelezi, K., & Buthelezi-Dube, N. (2022). Effects of long-term (70 years) nitrogen fertilization and liming on carbon storage in water-stable aggregates of a semi-arid grassland soil. *Heliyon*, 8(1). https://doi.org/10.1016/j.heliyon.2022.e08717.

Badan Pusat Statistik., (2024). *Luas Panen, Produktivitas, dan Produksi Padi Menurut Kabupaten/Kota di Provinsi Maluku [Harvested Area, Productivity, and Rice Production by Regency/City in Maluku Province], 2023*, BPS Provinsi Maluku, Ambon.

Cai, J., Shen, C., Ye, M., Huang, S., He, J., & Cui, D. (2023). Influencing factors of porosity and strength of plant-growing concrete. *Materials*, 17(1), 31.

Cheng, Q., Chen, X., Tao, M., & Binley, A. (2019). Characterization of karst structures using quasi-3D electrical resistivity tomography. *Environmental Earth Sciences*, *78*, 1-12. https://doi.org/10.1007/s12665-019-8284-2.

Crnobrna, B., Llanqui, I. B., Cardenas, A. D., & Panduro Pisco, G. (2022). Relationships between organic matter and bulk density in Amazonian peatland soils. *Sustainability*, *14*(19), 12070. https://doi.org/10.3390/su141912070.

Dermawan, D. A., Harisuseno, D., & Fidari, J. S. (2022). Estimasi laju infiltrasi berdasarkan kadar air, porositas, dan komposisi tanah di Sub DAS Lesti [Estimation of infiltration rate based on water content, porosity, and soil composition in the Lesti Sub-DAS]. *Jurnal Teknologi dan Rekayasa Sumber Daya Air*, *2*(2), 352-352. https://doi.org/10.21776/ub.jtresda.2022.002.02.28.

Doni, D., Ivansyah, O., & Muhardi, M. (2021). Penggunaan metode geolistrik untuk mengidentifikasi pengaruh pemupukan terhadap nilai resistivitas tanah [The use of geoelectric methods to identify the effect of fertilization on soil resistivity values]. *Prisma Fisika*, *9*(3), 263-270. https://doi.org/10.26418/pf.v9i3.51245.

Farooq, U., Gorczewska-Langner, W., & Szymkiewicz, A. (2024). Water retention curves of sandy soils obtained from direct measurements, particle size distribution, and infiltration experiments. *Vadose Zone Journal*, *23*(4), e20364. https://doi.org/10.1002/vzj2.20364.

Havlin, J.L., Tisdale, S.L., Nelson, W.L., & Beaton, J.D. (2014). *Soil Fertility and Fertilizers: An Introduction to Nutrient Management* (8th ed.). Pearson Education

Hillel, D. (1982). *Fundamentals of soil physics*. Academic Press.

Hovhannissian, G., Podwojewski, P., Le Troquer, Y., Mthimkhulu, S., & Van Antwerpen, R. (2019). Mapping spatial distribution of soil properties using electrical resistivity on a long term sugarcane trial in South Africa. *Geoderma*, *349*,56-67. https://doi.org/10.1016/j.geoderma.2019.04.036.

Iqbal, I., Mandang, T., & Sembiring, E. N. (2006). Pengaruh lintasan traktor tanpadan pemberian bahan organik terhadap pemadatan tanah dan keragaan tanaman kacang tanah [The effect of tractor traverse without and application of organic materials on soil compaction and peanut plant performance]. *Jurnal Keteknikan Pertanian*, *20*(3), 21778.

Jusoh, M. N. H., Syamsunur, D., Abd Rahman, N., Olisa, E., Rahim, A., & Md Yusoff, N. I. (2022). Soil parameters model prediction via resistivity value limit to shallow subsurface areas. *Shock and Vibration*, 2022(1), 3251250. https://doi.org/10.1155/2022/3251250.

Liu, Y., Zhang, Y., & Wang, X. (2024). Photosynthetic traits, water use and the yield of maize are influenced by soil water stability. *BMC Plant Biology*, 24, 59. https://doi.org/10.1186/s12870-024-05942-4.

Liu, G., Shohag, M., Hickey, L., Li, Y., & Tian, S. (2024). A practical guide for adjusting fertigation water pH in Specialty Crop Production. *Horticultural Sciences, 2024* (6). https://doi.org/10.32473/edis-hs1490-2024.

Liu, Y., Zhang, M., Li, Y., Zhang, Y., Huang, X., Yang, Y., ... & Jiang, T. (2023). Influence of nitrogen fertilizer application on soil acidification characteristics of tea plantations in karst areas of southwest China. *Agriculture*, 13(4), 849. https://doi.org/10.3390/agriculture13040849.

Loke, M. H., & Dahlin, T. (2002). A comparison of the Gauss–Newton and quasi-Newton methods in resistivity imaging inversion. *Journal of Applied Geophysics*, 49: 149-162. http://dx.doi.org/10.1016/S0926-9851(01)00106-9.

Lopes, I., de Lima, J. L., Montenegro, A. A., & Carvalho, A. A. D. (2025). Assessment of Water Retention and Absorption of Organic Mulch Under Simulated Rainfall for Soil and Water Conservation. *Soil Systems*, *9*(1), 4. https://doi.org/10.3390/soilsystems9010004.

Memon, M. B., Yang, Z., Qazi, W. H., Pathan, S. M., & Chalgri, S. R. (2024). Assessing soil bulk density, plasticity index, porosity, and degree of saturation through electrical resistivity using correlation analysis. *Malaysian Journal of Soil Science*, 28

Murni, P. (2009). Peningkatan pH tanah Podsolik Merah Kuning melalui pemberian abu dan hubungannya dengan aktivitas mikroorganisme pengikat Nitrogen [Increasing the pH of Red Yellow Podsolic soil through the addition of ash and its relationship with the activity of nitrogen-fixing microorganisms]. *Jurnal Biospesies*, 2(2), 18-20.

Niaz, A., Awan, A. M., Bibi, T., Rahim, S., Qureshi, J. A., Hameed, F., & Shedayi, A. A. (2021). A comparison between schlumberger and wenner configurations in delineating subsurface water bearing zones: A Case Study of Rawalakot Azad Jammu and Kashmir, Pakistan. *Int. J. Econ. Environ. Geol,* 12 (3): 25-31. https://doi.org/10.46660/ijeeg.Vol12.Iss3.2021.615.

Orzech, K., Wanic, M., & Załuski, D. (2021). The effects of soil compaction and different tillage systems on the bulk density and moisture content of soil and the yields of winter oilseed rape and cereals. *Agriculture*, *11*(7), 666. https://doi.org/10.3390/agriculture11070666.

Pownall, J. M., Hall, R., & Watkinson, I. M. (2013). Extreme extension across Seram and Ambon, eastern Indonesia: evidence for Banda slab rollback. *Solid Earth*, *4*(2), 277-314. https://doi.org/10.5194/se-4-277-2013.

Putra, P., Elpani, P., Fadhilah, A., & Ghony, M. A. (2023). Analisis perbandingan berat jenis tanah sampel batulempung dan batupasir pada titik bor MHY 52A [Comparative analysis of soil specific gravity of claystone and sandstone samples at drill point MHY 52A]. *Jurnal Ilmiah Teknik dan Sains*, 1(2), 73-78. https://doi.org/10.5897/SRE10.1036.

Reynolds, J. M. (1997). *An introduction to applied and environmental geophysics. In An introduction to applied and environmental geophysics*. Wiley-Blackwell.

Salufu, S. O., & Aigbedion, I. (2022) Effects of soil resistivity variation with depth on crop yield in a typical sedimentary terrain: a geophysical method application in agricultural practice. *Sumerianz Journal of Scientific Research*, 5 (4): 63-72. https://doi.org/10.47752/sjsr.54.63.72.

Santoso, P., Arman, Y., & Ihwan, A. (2015). Identifikasi perubahan nilai resistivitas tanah gambut akibat penyemprotan herbisida sistem kontak menggunakan metode geolistrik resistivitas konfigurasi dipole dipole [Identification of changes in peat soil resistivity values due to contact system herbicide spraying using the dipole-dipole configuration resistivity geoelectric method]. *Prisma Fisika*, *3*(3). https://doi.org/10.26418/pf.v3i3.13602.

Sonora, W. E., Harisuseno, D., & Fidari, J. S. (2022). Prediksi laju infiltrasi berdasarkan porositas tanah dan komposisi tanah [Prediction of infiltration rate based on soil porosity and soil composition]. *Jurnal Teknologi dan Rekayasa Sumber Daya Air*, 2(1), 291–303. https://doi.org/10.21776/ub.jtresda.2022.002.01.24.

Saputra, D. D., Putrantyo, A. R., & Kusuma, Z. (2018). Hubungan kandungan bahan organik tanah dengan berat isi, porositas dan laju infiltrasi pada perkebunan salak di Kecamatan Purwosari, Kabupaten Pasuruan [The relationship between soil organic matter content and bulk density, porosity and

infiltration rate in snake fruit plantations in Purwosari District, Pasuruan Regency]. *Jurnal Tanah dan Sumberdaya Lahan, 5*(1), 647-654. https://doi.org/10.21776/ub.jtsl.2018.005.1.1.

Syabawaihi, S., Sari, I. P., & Octalia, V. (2025). Analisis dampak perubahan iklim terhadap produktivitas perkebunan karet terhadap kesejahteraan petani di Kabupaten Musi Rawas [Analysis of the impact of climate change on rubber plantation productivity and farmer welfare in Musi Rawas Regency]. *INSOLOGI: Jurnal Sains dan Teknologi*, *4*(2), 189-198.

Syahputra, D., Rohmiyati, S. M., & Syah, R. F. (2024). Pengaruh kombinasi pupuk kandang dan dolomit terhadap bibit kelapa sawit (Elaeis Guineensis Jacq) di main nursery pada tanah masam [The effect of a combination of manure and dolomite on oil palm seedlings (Elaeis Guineensis Jacq) in the main nursery on acidic soil]. *Agroforetech*, *2*(3), 1346-1351.

Taruna, Y., Salampak, Yulianti, N., Yupi, H. M., Sustiyah, & Indrajaya, F. (2021). Pengaruh penyiraman air tanah terhadap perubahan sifat kimia tanah dan air gambut di Kalimantan Tengah [The effect of groundwater irrigation on changes in the chemical properties of soil and peat water in Central Kalimantan]. *Soilrens*, 19(1), 58–66.

Wang, N., & Zhang, T. (2024). Soil pore structure and its research methods: A review. *Soil and Water Research*, 19(1), 1-24. https://doi.org/10.17221/64/2023-SWR.

Widodo, W. (2023). DC resistivity and electromagnetic induction techniques for soil characterization in the agriculture land (Case Study in Cidadap, West Bandung, West Java). *Journal of Environmental and Engineering Geophysics*, 28(4), 197–208. https://doi.org/10.32389/JEEG23-004.

Zhang, N., Wang, M., & Wang, N. (2002). Precision agriculture—a worldwide overview. *Computers and electronics in agriculture*, *36*(2-3), 113-132. https://doi.org/10.1016/S0168-1699(02)00096-0.

Zhao, K., Xu, Q., Liu, F., Xiu, D., Ren, X., (2020): Field monitoring of preferential infiltration in loess using time-lapse electrical resistivity tomography. *J. Hydrol*. 591, 125278. https://doi.org/10.1016/j.jhydrol.2020.125278.